Chalcogenide Letters Vol. 12, No. 11, November 2015, p. 579 - 588

PbS THIN FILMS GROWTH WITH CBD AND PCBD TECHNIQUES: A COMPARATIVE STUDY

C.E. PÉREZ-GARCÍA, R. RAMÍREZ-BON, Y.V. VOROBIEV*
Cinvestav del IPN, Unidad Querétaro, Libramiento Norponiente 2000, Juriquilla, 76230, México.

PbS thin films were deposited by traditional chemical bath deposition CBD and CBD under UV radiation using a commercial UV-lamp (Photo CBD, or PCBD). The properties of both types of PbS films were analyzed by several techniques to determine the influence of the UV light during the film deposition process. We found that PCBD gives a significantly accelerated growth rate. The improvement in the deposition rate is because the UV radiation provides the energy needed to break the C-S bond in compound present in Chemical Bath, thus accelerating the formation of the PbS molecules, and in consequence decreasing the deposition time to attain specific film thickness.The films show an increase in the thickness compared to the films without UV radiation (from 200 nm to 747 nm for 5 hours deposition time). The optical, electrical and structural properties were different in the two cases, reflecting the difference in variation of porosity with deposition time. For CBD-made films the electrical resistivity is 4.1 Ω·cm, and for PCBD films it is 30 Ω·cm.

(Received July 18, 2015; Accepted November 9, 2015)

Keywords: Semiconductors; Thin Films; Chemical bath deposition, Photochemical Bath Deposition

1. Introduction

In recent years the essential part of research in semiconductors has been aimed to the application of them in photovoltaic cells [1] in order to find alternative energy production techniques that are clean and easy to obtain. Currently the majority of commercial solar cells are made from silicon, which has a high cost of production, stimulating the investigation of new materials that are easy to synthesize and with a low cost of production. The chalcogenide semiconductor thin films have been a viable option to replace monocrystalline silicon solar cells [2]. These films have the advantage of being simple to produce and have a low cost of production.

In particular the Lead Sulfide (PbS) is a semiconductor that have been studied for many applications like infrared detectors [3], transistors [4] and thin film solar cells [5–7].

In this work PbS films were grown at room temperature using two different techniques: Chemical Bath Deposition (CBD) and Photo Chemical Bath Deposition (PCBD) [8]. It should be noted that the most common technique to grow these films is CBD [8]–[11]. The PCBD technique was previously used for production of materials like CdS and ZnS [13–15]; it was found that morphology and structure of materials obtained by this method is essentially different from those characteristic for CBD-made samples. To our knowledge, there is only one publication that exposes the chemical bath under solar radiation and under tungsten incandescent lamp. They accelerate significantly the reaction increasing the temperature, giving a higher deposition rate [16]. On the other hand, M. Ichimura et al. used a high-pressure mercury-arc lamp, but in their case this lamp was necessary to maintain the reaction and not to accelerate it [17]; there are no publications on PbS made by PCBD using a UV lamp, so we expect that comparison of the materials obtained by these two methods will bring useful information.

*Corresponding author: vorobiev@qro.cinvestav.mx

2. Experimental

2.1.Thin films deposition

The substrates used in the present work were Corning microscope glass slides (75mmx25mm of 2mm thickness) and Silicon wafer (15mmx15mmx 0.28 mm) for Infrared (IR) spectroscopy measurements.

2.1.1.PbS films by CBD technique

PBS films were grown by chemical bath deposition (see [7] for details) at room temperature (25ºC), where the substrate was immersed vertically in a solution of 100 ml containing: 5ml 0.5M of lead acetate $Pb(C_2H_3O_2)_2$ as source of Pb^+ ions; 5ml 2M of sodium hydroxide (NaOH); 6ml 1M of thiourea $CS(NH_2)_2$ to produce S^- ions; 2ml 1M of Triethanolamine (TEA) as complexing agent and water, the growing was made in darkness, then, the substrate was removed using different times: 60 min, 90 min, 120 min, 180 min, 240 min and 300 min. The resulting films were homogeneous and well adhered to the substrate with like-mirror dark surface.

2.1.2. PbS films grown by PCBD

PbS films grown by PCBD were prepared following the same procedure used for the CBD technique described in the section 2.1.1. But, for this procedure, the beaker container was irradiated with UV-light during the immersion times using a UV-lamp of 11 Watts with a total irradiation of 20 W/m^2 and the main wavelength of 335 nm.

2.2 Structural and optical characterization

The surface morphology of the films and the average roughness were determined using an Atomic Force Microscopy (AFM) and Scanning Electron Microscopy (SEM) imaging. The AFM measurements were performed at 2% of relative humidity and 15ºC with a commercial SPM system, a Brunker/Veeco/Digital Instruments Nanoscope IV Dimension 3100, operating in a tapping mode and using Budget Sensors Cr/Pt-coated silicon probes (ElectriTap300-G). The particle size of the films was determined using a scanning electron microscope (Philips-FEG-XL30), a layer of gold was evaporated on the films previous to the SEM measurements.

X-Ray diffraction (XRD) patterns of the PbS films were recorded in a Rigaku D/MAX-2000 diffractometer, using Cu-Kα radiation. The average crystallite size of the films was evaluated using the software (JADE) supplied, with Scherer formula.

Optical transmittance and reflectance of the films were obtained using a spectrophotometer Film-Tek (TM-3000) in the spectral range of 240 to 840 nm (UV-VIS region). The index of refraction (n) and extinction coefficient (k) were obtained using the Film-Tek software. The energy band gap (Eg) of the films was calculated from the transmittance spectra obtained using a FTIR spectrometer Perkin Elmer GX, in the range of 400 to 7800 nm corresponding to NIR and Medium IR region.

2.3. Electrical characterization

To obtain the resistivity of the films, a pair of colloidal silver paint electrodes were applied on the films, then, a current (I) vs voltage (V) measurements were made with a Semiconductor Parameter Analyzer Agilient 4155C.

3. Results and discussion

3.1. Reaction mechanism

The CBD reaction involves two steps, nucleation and particle growth. The film growth can take place either by ion-by ion condensation of materials or by adsorption of colloidal particles from the solution on the substrate [18]. The PCBD reactions, for this study, follow the same pathway that the CBD one, where the UV-lamp provides energy to the reaction (see explanation

below). The CBD reaction involves two reactions mechanism, the first one consist of simple cluster (hydroxide) mechanism [19], which occurred when the formation of the lead hydroxide takes place. Pb^{2+} ion results from $Pb(OH)_2$ at basic pH in aqueous solution; TEA inhibit the precipitation of $Pb(OH)_2$ and allows the hydroxide to break the double bond C=S of thiourea yielding S^{2-} ion. Coupling of Pb^{2+} and S^{2-} ions renders PbS. The energy required to break C=S bond is 4.93 eV, this energy corresponds to photon within the UV region. When the PbS exceeds the solubility constant (Ks), the PbS starts to precipitate, see Fig. 1.

The second reaction mechanism, ion by ion mechanism, involves the hydrolysis of the thiourea [20]. This reaction mechanism generally occurs at acid pH, but the amphoteric behavior of water triggers the spontaneous hydrolysis of thiourea. For this reaction to occur it is also necessary to break the C-S bond (that is, hydrolysis of the thiourea, see Fig. 2). The energy needed to break this bond is 3.81 eV. As in the simple cluster mechanism, the energy necessary to cleave bonds involved in the reaction is within the UV spectral region; in this way UV lamp provides energy to the reaction thus further promoting the formation of the PbS.

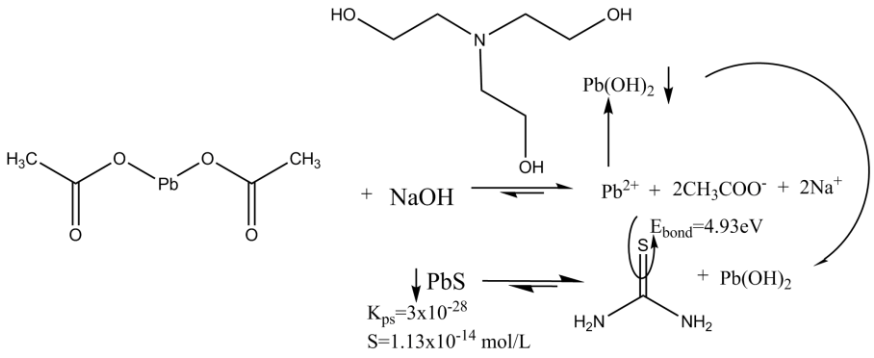

Fig. 1. Simple cluster reaction mechanism

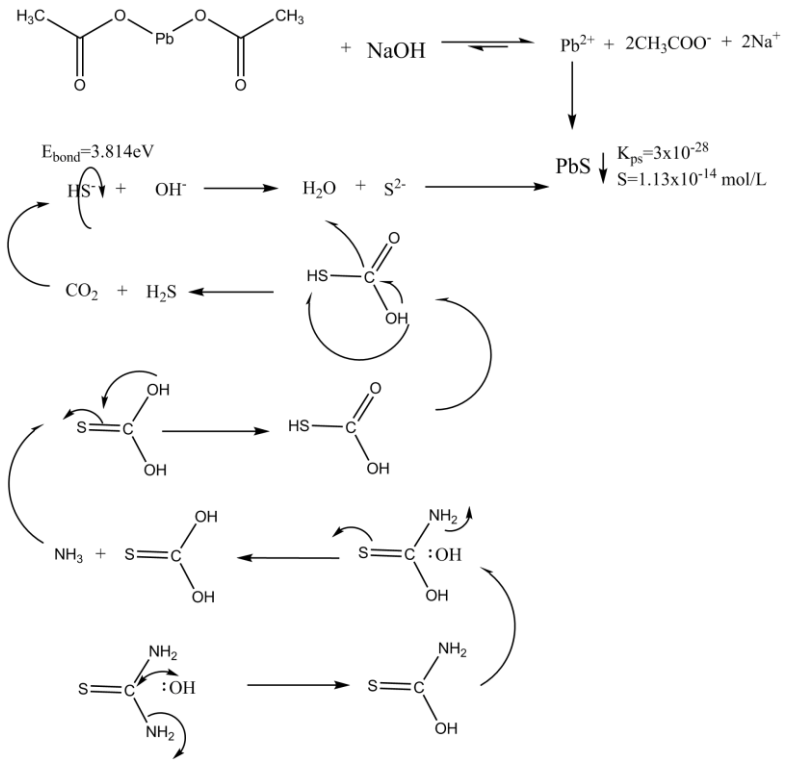

Fig. 2. Ion by ion mechanism reaction

3.2. Thickness determination

Fig. 3 (stars) shows the thickness for the PbS films grown with CBD, the thickness increases with the deposition time from 58 to 200 nm. For the PbS films grown with PCBD (squares) in Fig. 3, it is observed that the thickness increases with deposition time up to 750 nm until 5 hours, later the thickness decreases down to 400 nm for 7 hours of deposition time. We observe that under the UV illumination we obtain the largest thickness; we assume that this increase in thickness is due to the UV effect in breaking the molecular bonds as discussed above. The thickness decrease in PCBD case after 6 hrs can be due to the precursors solutions was exhausted.

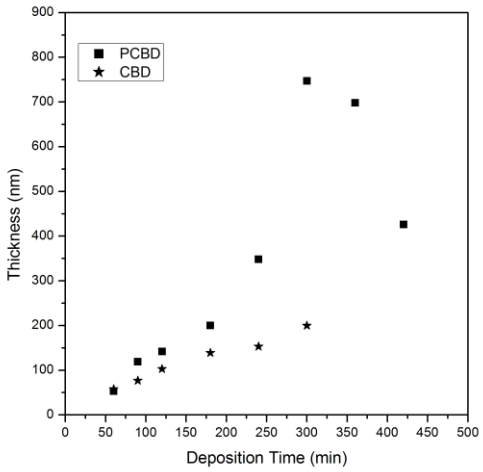

Fig. 3.Thickness vs deposition time: stars for CBD films and squares for PCBD films

3.3. Morphology determination

Fig. 4 shows the AFM and SEM images for the CBD film, for the films in fig. 4a) and 4c), a compact surface is observed with a particle size of 173.9 nm. This compact surface was observed for all the different deposition times. For PCBD films (fig 4 b) and d)) a regular and homogeneous surface can be observed with average particle size of 154.9 nm; these characteristics can be observed for all depositions times. The PCBD films show a more compact material and smaller particles, with fewer aggregates than the CBD ones. Fig. 5 shows the roughness of the films, we observe that for CBD films we obtain a linear dependence with the deposition time, whereas for PCBD the dependence is different: roughness as well as thickness initially grow quicker than in CBD case, later saturates.

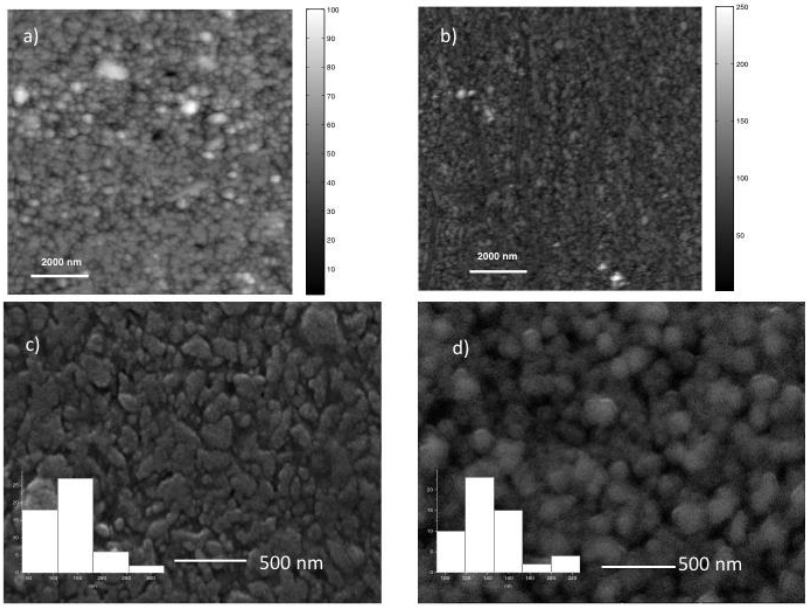

Fig. 4. a) AFM image and c) SEM image for CBD films deposited for 3 hrs, b) AFM image and d) SEM image for PCBD films deposited for 2 hrs

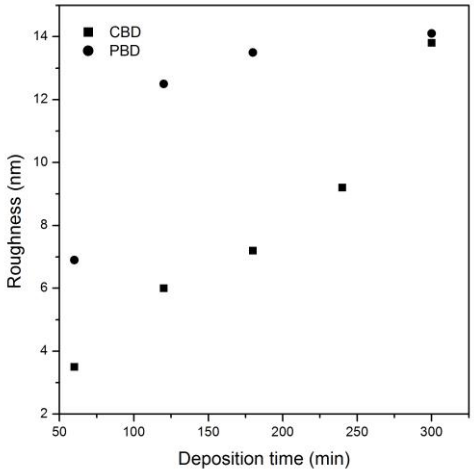

Fig. 5. Roughness vs deposition time for CBD and PCBD deposition

3.4. Structural Analysis

Fig. 6 shows the XRD pattern of a film of PbS deposited by CBD. The XRD peaks are well defined and are identical to the mineral Galena (PbS, PDF 05-0592). This pattern appears for the films after 60 minutes of deposition, the intensity of the peaks increases with the deposition time. In Fig. 6 the XRD pattern for the PCBD film is shown; again we obtain XRD peaks identical to the mineral Galena, same as the CBD ones. Films with 6 and 7 hours of deposition time were made with the objective to observe if the crystallinity is conserved. For PCBD case, crystalline films can be obtained at longer times of deposition, but there is a decrease in thickness.

The crystallite size for both different deposition methods was 21.36 nm. This size is different from the one obtained in micrographics with SEM, this is due to the fact that in SEM the aggregates are observed.

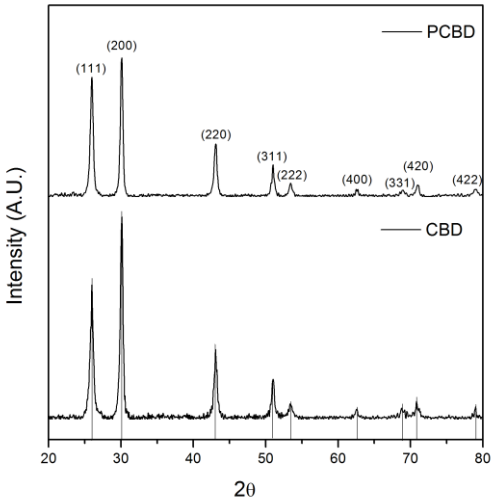

Fig. 6 XRD patterns for CBD and for PCBD films

3.5. Optical Characterization

In fig. 7 the transmittance (T) and reflectance (R) spectra for PbS films are presented, the red lines show the T and R for CBD grown during 3 hrs and black lines show the T and R for PCBD films deposited during 2 hrs.

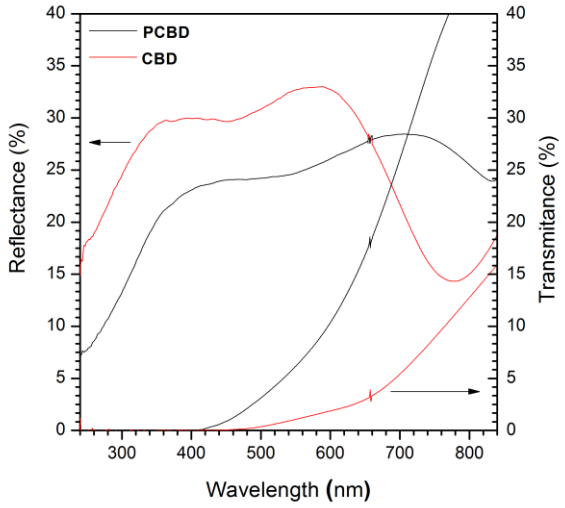

Fig. 7. Reflectance and Transmittance spectra for CBD film deposited during 3 hr and for PCBD film deposited during 2 hr

In fig. 8 we observe the optical constants for the films grown with the two techniques, red lines show the spectra for CBD sample for 3 Hr of deposition time and black lines show the spectra for PCBD with 2 Hr of deposition time. These deposition times were chosen because the corresponding films have similar thickness. The films deposited by CBD show the lower transmittance, which is the ideal for use as p-type material in a solar cell.

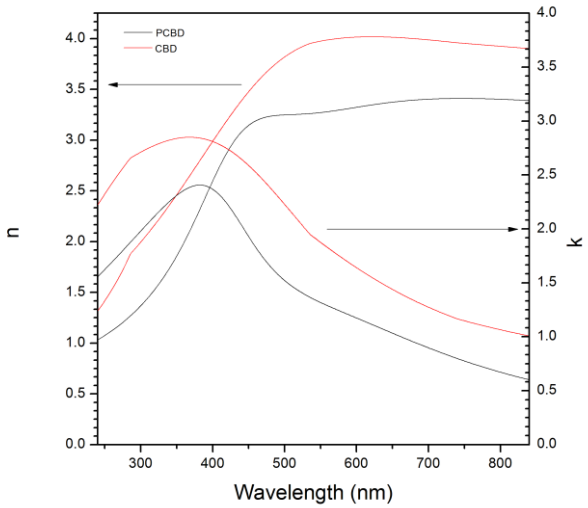

Fig. 8. n and k constants for CBD film deposited during 3 hr and for PCBD film deposited during 2 hr

The values of the Eg for the films were determined from the transmittance spectra. The plots of the $(OD*E)^2$ versus E spectra (Fig. 9 a)) in the IR absorption region were fitted to the model for direct allowed transitions between parabolic energy bands, where, OD is the optical density and E is the photon energy. Fig. 9 b) shows the graph of energy band gap values for CBD, in this image we observe that the Eg decreases from 0.52 to 0.38eV while the deposition time increases, and for the sample with 5 hr of deposited time an abrupt decrease is seen. In Fig. 8c) we see that for PCBD films the Eg increases from 0.32 to 0.52 eV as the deposition time increases.We observe that the band gap edge in both deposition techniques presents a blue shift; this is due to nanopores in the material (see [21] for more details).

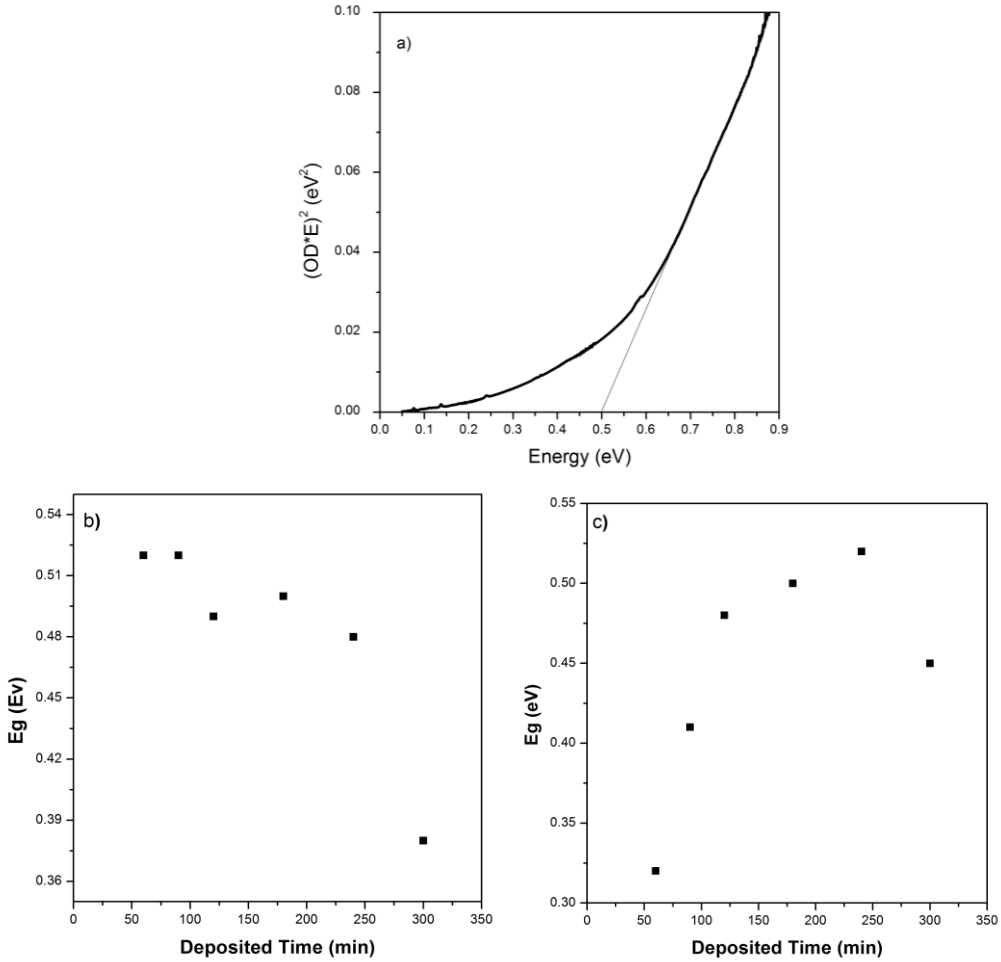

Fig. 9 a) Diagram used to determine band gap of PbS CBD sample with growth time of 3 hr. b) Eg values for CBD at different deposition times. c) Eg values for PCBD at different deposition times

We see that a blue shift is quite big in both cases, which means that small pores prevail (around 6 nm in size, according to estimations made in [20]). The character of gap variation with deposition time in CBD and PCBD cases is different: Eg decreases with time in the first case, and increases with quick saturation in the second one. Our conclusion is that the slow growth by CBD produces denser material with smaller porosity at larger deposition time, whereas PCBD gives thicker film with approximately constant porosity. This conclusion agrees with optical constants data: larger refractive index in CBD-made samples confirms smaller porosity. Electrical measurements (below) also confirm that.

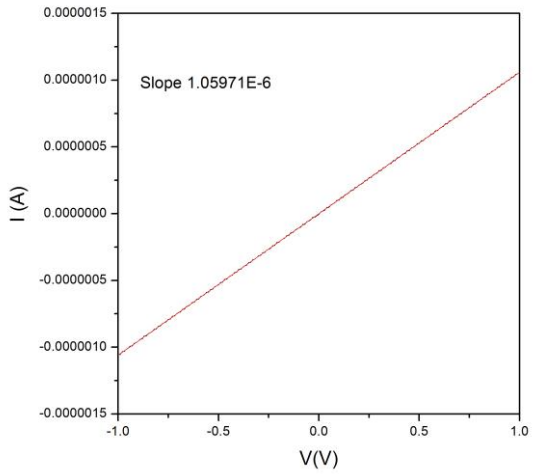

Fig. 10. I - V curve used to determine the resistivity of a PbS film deposited by CBD during 4 hr

3.6. Electrical Characterization

The resistance of the films was obtained from the slope of the I vs V curves, Fig. 10 Using the area and thickness of the films, the resistivity (ρ) was calculated as in [22],

$$\rho = \frac{xW}{L} R \tag{1}$$

where L is the distance between the contacts, x is the longitude of the contact and W is the thickness of the film. For CBD films the resistivity is 4.1 Ω·cm, and for PCBD films it is 30 Ω·cm; these results correspond to the resistivity values of semiconductor films fabricated by CBD [13].

4. Conclusions

Based on the results obtained in this work we recommend the use of UV-light during the CBD deposition to reduce the deposition time and increase the thickness of the films. This technique could be a good option to grow thicker films in less time deposition of materials that involve Thiourea like ion S^{2-} precursor.

Acknowledgements

The authors acknowledge the financial support of CONACYT, Project No. 152513. C.E. Pérez-García wish to thank CONACYT for her scholarship. We acknowledge the technical assistance of: C.A. Avila-Herrera, M. A. Hernández-Landaverde, J.E. Urbina-Alvárez, R.A. Mauricio-Sánchez, I.R. Chávez-Urbiola and F.J. Flores-Ruiz.

References

[1] M. Afzaal, P. O'Brien, J. Mater. Chem. **16**, 1597 (2006).
[2] P.K. Santra, P. V. Kamat, J. Am. Chem. Soc. **135**, 877 (2013).
[3] C.J. Baddiley, J. Ring, Infrared Phys. **17**, 405 (1977).
[4] I.E. Morales-Fernández, M.I. Medina-Montes, L. A. González, B. Gnade, M. A. Quevedo-López, R. Ramírez-Bon, Thin Solid Films. **519**, 512 (2010).
[5] P. Nair, Sol. Energy Mater. Sol. Cells. **52**, 313 (1998).

[6] J.J. Valenzuela-Jáuregui, R. Ramírez-Bon, a. Mendoza-Galván, M. Sotelo-Lerma, Thin Solid Films. **441**, 104 (2003).
[7] J. Hernández-Borja, Y.V. Vorobiev, R. Ramírez-Bon, Sol. Energy Mater. Sol. Cells. **95**,1882 (2011).
[8] I.. Chávez-Urbiola, Y.V. Vorobiev, R. Ramírez-Bon, Sol. Energy Mater. Sol. Cells. in print (2015).
[9] A. Gaiduk, P. Gaiduk, A. Larsen, Thin Solid Films. **516**, 3791 (2008).
[10] K.M. Gadave, S.A. Jodgudri, C.D. Lokhande, Thin Solid Films. **245**, 7 (1994).
[11] S. Seghaier, N. Kamoun, R. Brini, A. B. Amara, Mater. Chem. Phys. **97**, 71 (2006).
[12] M. Najdoski, B. Mincerva-Sukarova, A. Drake, I. Grozdanov, C.J. Chunnilal, J. Mol. Struct. **349**, 85 (1995).
[13] F. Goto, M. Ichimura, E. Arai, Japanese J. Appl. Physics, Part 2 Lett. 36 (1997).
[14] M. Ichimura, F. Goto, Y. Ono, E. Arai, J. Cryst. Growth. **198-199**, 308 (1999).
[15] M. Gunasekaran, R. Gopalakrishnan, P. Ramasamy, Mater. Lett.,67–70, 58 (2004).
[16] P.K. Nair, V.M. Garcia, a B. Hernandez, M.T.S. Nair, J. Phys. D. Appl. Phys. **24**,1466 (2000).
[17] M. Ichimura, T. Narita, K. Masui, Mater. Sci. Eng. B Solid-State Mater. Adv. Technol. **96**, 296 (2002).
[18] R.S. Mane, C.D. Lokhande, Mater. Chem. Phys. **65**,1 (2000).
[19] S.M. Pawar, B.S. Pawar, J.H. Kim, O.S. Joo, C.D. Lokhande, Curr. Appl. Phys. **11**,117 (2011).
[20] H. Lima-Lima, O. Portillo-Moreno, Superf. Y Vacio. **21**, 21 (2008).
[21] Y. V Vorobiev, P.P. Horley, J. Hernández-Borja, H.E. Esparza-Ponce, R. Ramírez-Bon, P. Vorobiev, et al., Nanoscale Res. Lett. **7**, 483(2012).
[22] K.C. Preetha, T.L. Remadevi, Phys. B Condens. Matter. **407**, 4173 (2012).